FIRST FREQUENCY MAPS FOR PROBING THE NON-LINEAR DYNAMICS OF SOLEIL

Laurent S. Nadolski*, P. Brunelle, J-P. Lavieville, P. Lebasque, A. Nadji, and M-A. Tordeux
Synchrotron SOLEIL, Gif-sur-Yvette, France

Abstract

SOLEIL is a 2.75 GeV third generation synchrotron light source delivering photons to beam-lines since January 2007. With a 3.7 nm.rad horizontal emittance, its optics is based on a strong focusing lattice. Large on- and off-momentum apertures are required in order to provide good injection efficiency and as large as possible Touschek beam lifetime. It is then fundamental to be able to understand the limitations of these key figures. In order to probe the transverse non linear dynamics two pinger magnets have been installed into the injection straight section during the summer 2007. In this paper, their calibration will be described. Then first comparisons between modeled and real machine will be given for betatron tune-shifts with amplitudes and frequency maps. To end the non-linear impact of insertion devices on beam dynamics will be discussed.

EXPERIMENTAL SETTING

Pinger magnets

Since August 2007, the 12 meter long injection straight section (SS) of the SOLEIL storage ring is equipped with one horizontal (H) and one vertical (V) machine study kickers (so-called pinger magnets). These two devices deliver a kick to the electron beam (e-beam) over one single turn: the plateau of the horizontal (vertical) pulse is 420 ns long (456 ns) whereas the revolution period is 1.2 μs. Maximum pulse amplitude is 2.8 mrad in H- and 1.2 mrad in V-plane enabling to kick the e-beam up to the physical aperture (see [1] for technical details on the machine study kickers).

The pingers have an excellent reproducibility (10^{-3}) and linearity of the magnetic field with the control voltage. Figure 1 displays the calibration on the pinger versus the amplitudes based on the magnetic measurements. Theses values have been cross checked carefully using the e-beam and the movable scrappers.

Beam Position Monitors (BPMs)

Thanks to their Libera electronics, the 120 BPMs can run at 10 Hz and 10 kHz rates for fast feedback operation as well as 846 kHz in turn-by-turn acquisition [2]. Libera modules present a H to V crosstalk that has been evaluated during a careful measurement campaign for appropriate corrections (2.5% RMS over all Liberas). The standard filtering, optimized for the slower acquisition rates does not fully decouple the position of a specific turn from its previous and following ones. A new filter isolating each turn position has been tested and will be implemented in the coming months. The BPM electrode geometry was optimized for reaching 0.2 μm RMS resolution for user operation (for low amplitudes). Because of the large ratio between the H- and V- BPM dimensions (82x25 mmxmm), the usual difference-over-sum formulas yields non-linearities outside a $\pm 4\,mm$ horizontal beam position range and saturates at about 6 mm. In the linear region, the BPM resolution is better than 3 μm RMS for turn by turn measurement. A strip-line BPM presently used as a H-and-V tune kicker can provide better resolution and linearity.

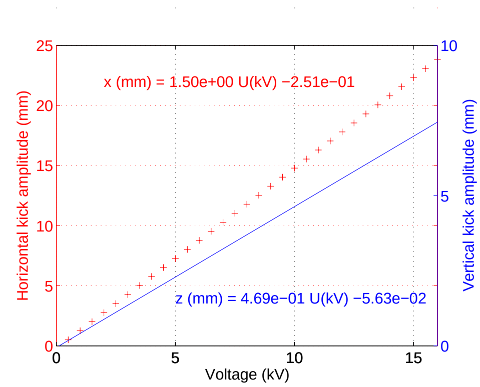

Figure 1: Linearity of the field integral delivered by both pinger magnets. The amplitudes are expressed in mm at the middle of the injection straight section.

Machine Settings

Both pinger magnets are triggered together with the BPMs for exploring the dynamics aperture of the storage ring. The experimental settings consist in storing 10 mA in 34 subsequent bunches (97 ns). This has been optimized in order to get a good enough signal to noise ratio without triggering collective effects which could spoil the measurements (e.g. by modifying the beam decoherence time or exciting intra-bunch instabilities).

MODELING THE STORAGE RING TRANSVERSE BEAM DYNAMICS

The storage ring optics is based on a modified Chasman-Green lattice with distributed H-dispersion to reach a 3.7 nm.rad emittance. Tracking is performed using the Tracy II 4th order integrator code [3]. On top of the bare lattice are added measured multipole errors for all the magnets modeled as thick elements (Tab. 1), the fringe field of the dipoles, the tilt errors of the dipole edges, and 1% coupling generated by randomly rotating the quadrupoles [5]. The quadrupole fringe field (QFF) will be introduced in the

* nadolski@synchrotron-soleil.fr

Table 1: List of multipole errors introduced into the lattice.

Dipole multipoles		**Sextupole multipoles**	
$2n$–poles	@ 20 mm	$2n$–poles	@ 32 mm
6	$-3.0\,10^{-4}$	18	$-4.7\,10^{-4}$
8	$+2.0\,10^{-5}$	30	$-9.0\,10^{-4}$
10	$-1.0\,10^{-4}$	42	$-20.9\,10^{-4}$
12	$-6.0\,10^{-5}$	54	$+0.8\,10^{-4}$
14	$-1.0\,10^{-4}$		
Short quad. multipoles		**Long quad. multipoles**	
$2n$–poles	@ 30 mm	$2n$–poles	@ 30 mm
6	$-1.6\,10^{-4}$	6	$+2.9\,10^{-4}$
8	$-3.4\,10^{-4}$	8	$-8.6\,10^{-4}$
12	$+2.4\,10^{-4}$	12	$+0.7\,10^{-4}$
20	$+0.7\,10^{-4}$	20	$+1.9\,10^{-4}$
28	$+0.9\,10^{-4}$	28	$+1.0\,10^{-4}$
H-corrector multipoles		**V-corrector multipoles**	
$2n$–poles	@ 35 mm	$2n$–poles	@35 mm
10	$+0.430$	10	-0.430
14	$+0.063$	14	$+0.063$
22	-0.037	22	$+0.037$

near future. For all the simulations, the physical aperture is taken into account all around the ring. The BPM turn by turn data are analyzed using the Frequency Map Analysis (FMA) (see ref. [4] and references therein) over 258 turns using a Hanning window. Recording an experimental frequency map of 40x12 points requires today 25 min.

BARE LATTICE

The working point of the bare lattice is $(\nu_x, \nu_z) = (18.20, 10.30)$ with a 0.3% total coupling value during the experiments.

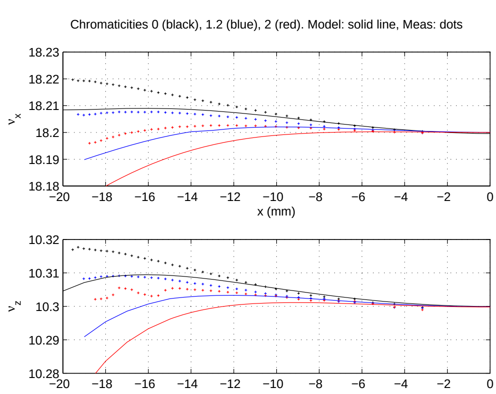

Figure 2: Bare lattice: Model (solid lines) vs. measurements (dotted lines): Comparison of the tune-shifts with H-amplitude for 0 (black), 1 (blue) and 2 (red) units of chromaticities in both planes.

Figure 2 displays the comparison of the tune-shifts with the H-betatron amplitudes for the bare lattice and 3 values of the chromaticities. At large H-amplitudes the systematic discrepancy between the e-beam measurements and the model (solid lines) shows a second order dependance. This could originate from the pseudo-octupole of QFF of the quadrupole magnets. Using analytical formula [6], the induced QFF tune-shift is always positive with two main contributions: one due to the quadrupole geometry and one proportional to the square of the QFF length. Figure 3 shows measured data corrected by the QFF, the agreement is much better.

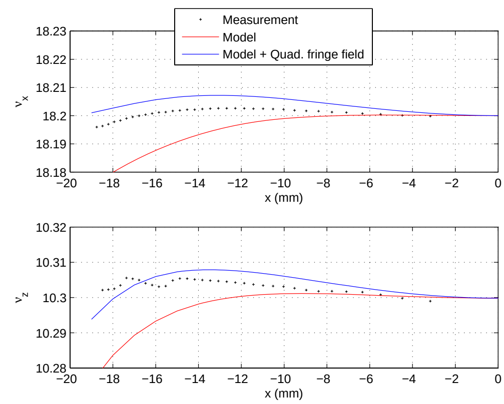

Figure 3: Tune-shifts with H-amplitude: measurement (dots), model without (red) and with QFF (blue) for $(\xi_x\, \xi_z) = (2, 2)$.

Concerning the measured dynamics aperture (DA), the agreement is pretty good with the simulation as shown by Fig. 4-left performed with chromaticity values $(\xi_x\, \xi_z) = (0, 0)$. All data are plotted at the middle of the injection straight section. The physical limitation is given by the position of the Eddy current septum (-20 mm). For the vertical plane at large H-amplitudes, the DA shrinks slightly more than expected. A beam lossy area is observed around $x = -6$ mm in H-plane and $z = 2.5$ mm in V-plane, related to the resonance $\nu_x - 4\nu_z = -23$ as observed on the frequency map (Fig. 4-right). Measured FMA differs from model for $x > 10$ mm without QFF. The experimental vertical tune-shift is significantly less pronounced.

MACHINE WITH INSERTION DEVICES

In this section, preliminary results concerning the nonlinear effects induced by the insertion devices (IDs) are given (see also [7]). For the ID modeling, 2D-kick maps from RADIA code [8] have been interfaced with the Tracy II tracking code.

In-vacuum Undulators: U20 Combined Effect

Figure 5-left displays the measured DA with 3 in-vacuum U20 IDs, at magnetic minimum gap value (5.5 mm) and for the nominal chromaticities $(\xi_x, \xi_z) =$

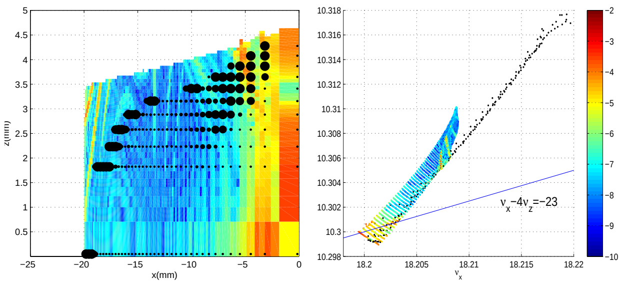

Figure 4: Bare lattice DA (left) and FMA (right) at zero chromaticities: measured DA data as black circles whose sizes are proportional to the relative beam loss each time the beam is kicked. Color code (for modeled data) is related to beam orbit diffusion rate.

$(2, 2)$, used in daily operation for the multi-bunch filling pattern. DA shrinks by 6 mm in H-plane, with a value just large enough for injection ($x = -10$ mm). The reduction in V-plane is less significative. Experimental FMA does not point out any strong variations of the tune-shifts with respect to the bare machine. The combined effect of 3 such IDs impacts drastically the beam performance: the injection efficiency drops down to 50%, the beam life-time is reduced by 33%.

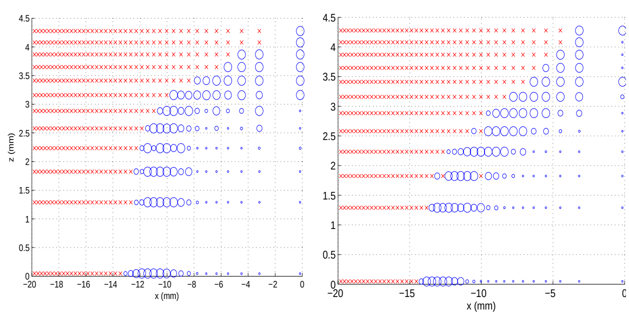

Figure 5: Experimental DA reduction. Effect of 3 in-vacuum undulators closed to minimum gap (left), and effect of HU640 in VL mode (right). Blue circles indicate beam losses, red crosses unstable beam.

Electromagnetic Undulator: HU640

HU640 is a 10 m long electromagnetic ID with very low field (0.1 T) with which no impact on the beam dynamics was expected [7]. Data for the worst configuration case of HU640, namely the vertical linear (VL) polarization mode, are here presented. The measured FMA (Fig. 6) reveals a strong reduction of the DA (Fig. 5-right) in both planes, leading to a 35% injection efficiency reduction for VL undulator mode. Tune-shifts with amplitude show strong contributions from higher multipoles, with a larger extension in tune space than for the bare lattice case. The beam seems to suffer from the strong dependence of the field integrals with the transverse coordinates unpredicted by the model. No clear resonance excitations are identified up to now (more refine data treatment is under way).

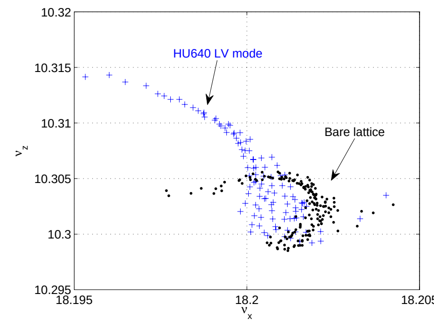

Figure 6: Frequency maps at$(\xi_x, \xi_z) = (2, 2)$: bare lattice (black) and VL-mode of HU640 (blue).

CONCLUSION AND PERSPECTIVES

The first measurements of DAs and FMAs reveal that the model is not perfectly matched to the real machine. Nevertheless, the DA limitations are closed to the expected values mostly given by the physical aperture. Integration of quadrupole fringe field in Tracy II tracking code will be done in the forthcoming weeks.

In the presence of IDs, the results are more difficult to interpret. If the effect of combined U20 undulators was expected in term of DA and lifetime, the HU640 large impact on the injection efficiency and the beam-lifetime was not predicted. This effect is not yet understood. Next step will be to retrofit the HU640 model.

Next series of experiments will also incorporate exploring the off-momentum dynamics.

REFERENCES

[1] P. Lebasque et al., “Construction of the two Machine Study Kickers and Improvement on Pulsed Magnetic Systems at SOLEIL”, these proceedings.

[2] N. Hubert et al., “The SOLEIL BPM and Orbit Feedback Systems”, DIPAC’07, Venice, 2007.

[3] Soleil version of Tracy II code.

[4] J. Laskar, “Fequency Map Analysis and Particle Accelerators”, Portland, PAC’03, 2003, pp. 378-382.

[5] P. Brunelle et al., “Magnetic Measurement Results of the Dipoles, Quadrupoles and Sextupoles of the SOLEIL Storage Ring”. EPAC’06, Edinburgh, 2006, pp. 3278-3280.

[6] F. Zimmermann, “Tune shift with Amplitude induced by quadrupole Fringe Fields”, CERN-SL-2000-009 AP, Neutrino Factory Note 18.

[7] P. Brunelle et al., “Experimental Characterization of the Insertion Device Effects on the Beam Dynamics at SOLEIL”, these proceedings.

[8] O. Chubar et al., “A 3D Magnetostatics Computer Code for Insertion Devices”, Journal of Synchrotron Radiation, 1998, Vol. 5, p. 481.